atmosphere

Supplementary Materials:

Jiayi Hou [1,2], Zheng Fang [1,2] and Xin Geng [1,2,3,*]

[1] CIC-FEMD/ILCEC, Key Laboratory of Meteorological Disaster of Ministry of Education (KLME), Nanjing University of Information Science and Technology, Nanjing 210044, China
[2] School of Atmospheric Science, Nanjing University of Information Science and Technology, Nanjing 210044, China
[3] Division of Environmental Science and Engineering, Pohang University of Science and Technology, Pohang 37673, Republic of Korea
* Correspondence: gengxin@nuist.edu.cn

This document contains six Supplementary figures with legends. The context and relevance of these figures are mentioned in the main text where appropriate.

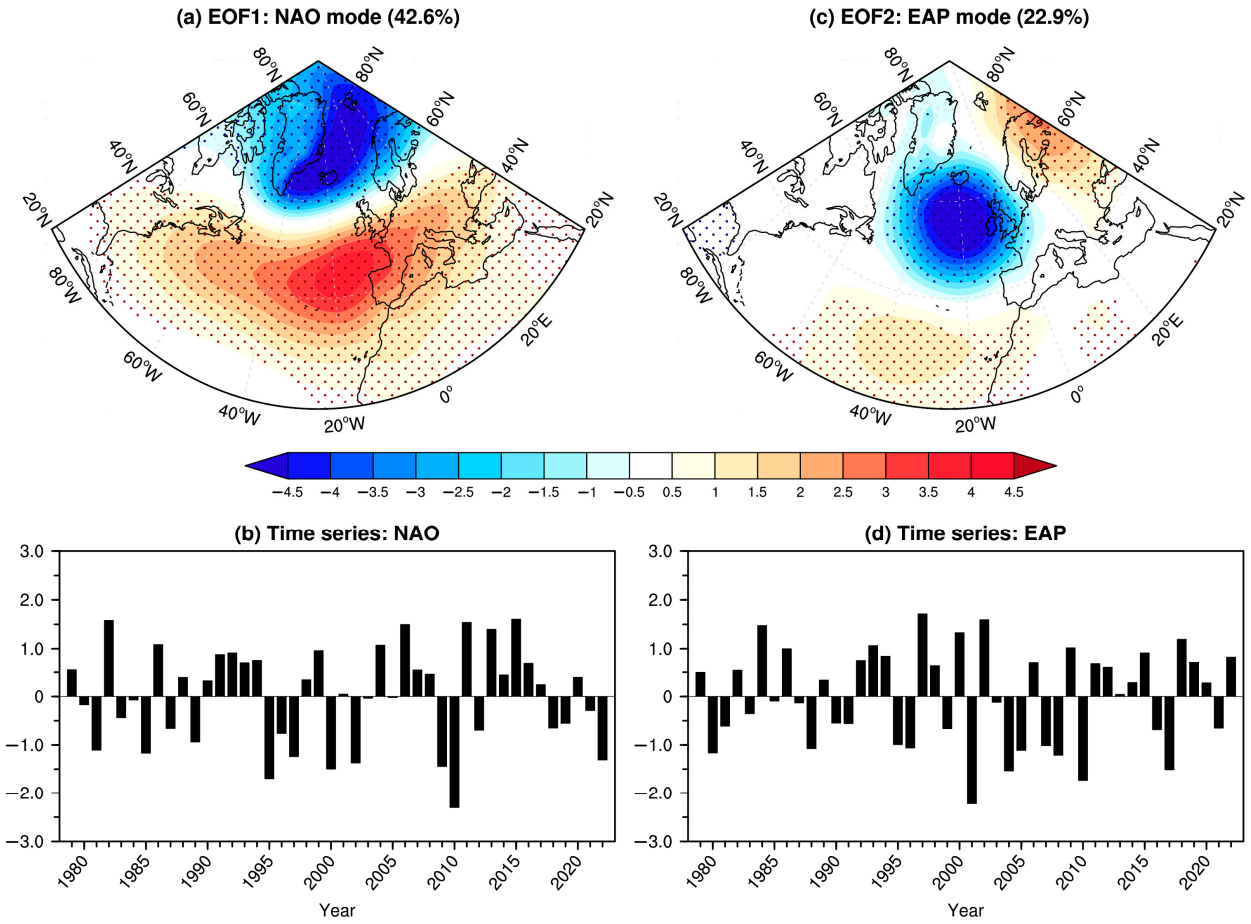

Figure S1. The (**a**) first and (**c**) second EOF spatial patterns (shading in hPa) and the corresponding (**b**) first and (**d**) second normalized time series (representing the NAO and EAP indices, respectively) of the early winter SLP anomalies in the North Atlantic region during 1979–2022 based on the NCEP/NCAR reanalysis dataset. The percentages in (**a**) and (**b**) are the variability explained by the corresponding EOF. The dots in (**b**) indicate the anomalies that exceed the 95% confidence level.

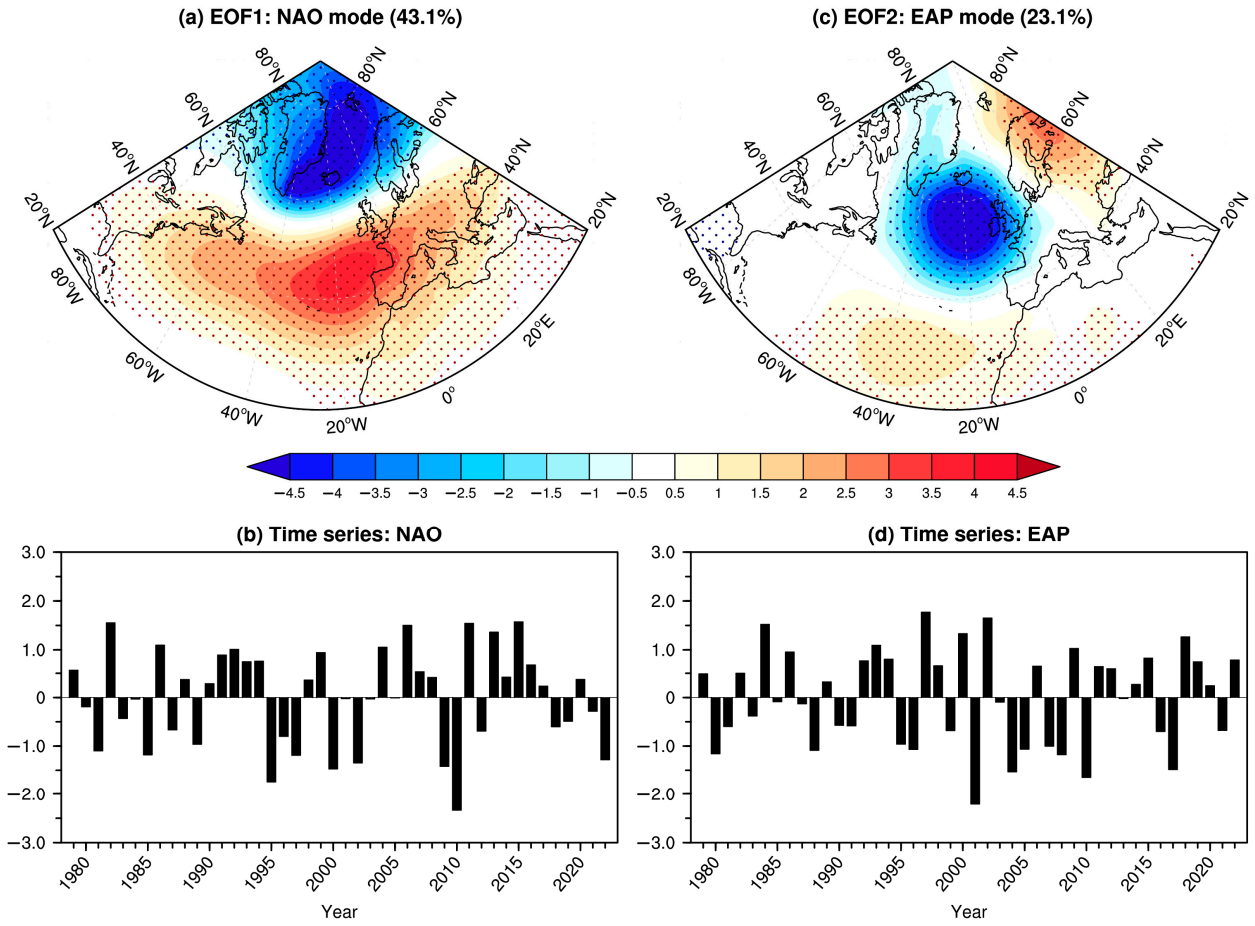

Figure S2. The same as Figure S1 but for the results calculated based on the JRA-55 Reanalysis dataset.

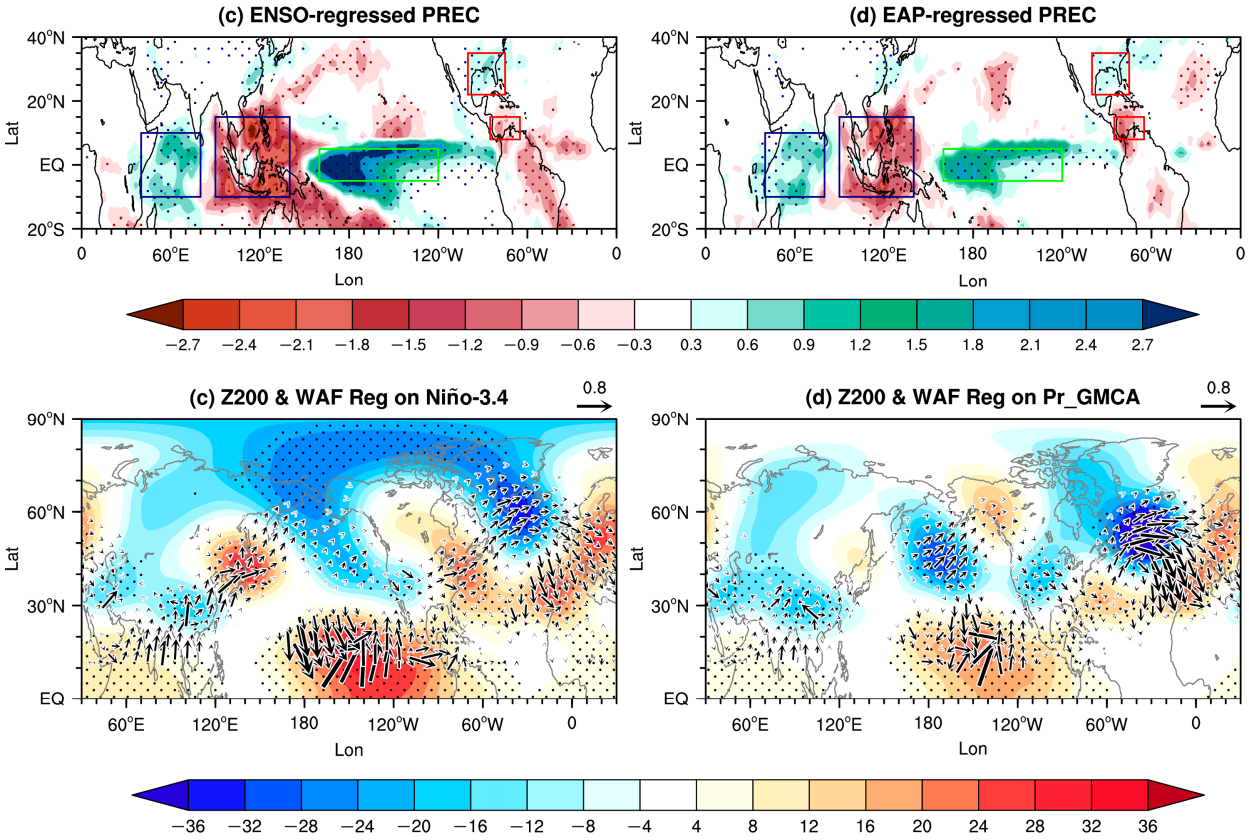

Figure S3. Regression coefficients of the early winter tropical precipitation anomalies (calculated based on the CMAP precipitation dataset, shading in mmday^{-1}) with respect to the (**a**) DJF Niño-3.4 and (**b**) early winter EAP indices. Regression coefficients of the early winter 200-hPa geopotential height anomalies (shading in m) and the associated anomalous wave activity flux (WAF, vectors in m^{2}s^{-2}) with respect to the (**c**) DJF Niño-3.4 and (**d**) early winter Pr_GMCA (calculated based on the CMAP precipitation dataset) indices. The dots indicate the anomalies that exceed the 95% confidence level. The navy, green and red boxes in (**a**) and (**b**) mark the domains used to define the Pr_TWEIO, Pr_CP and Pr_GMCA indices, respectively. The anomalous WAF flux in (**c**) and (**d**) is shown only when its magnitude is larger than 0.1 m^{2}s^{-2}.

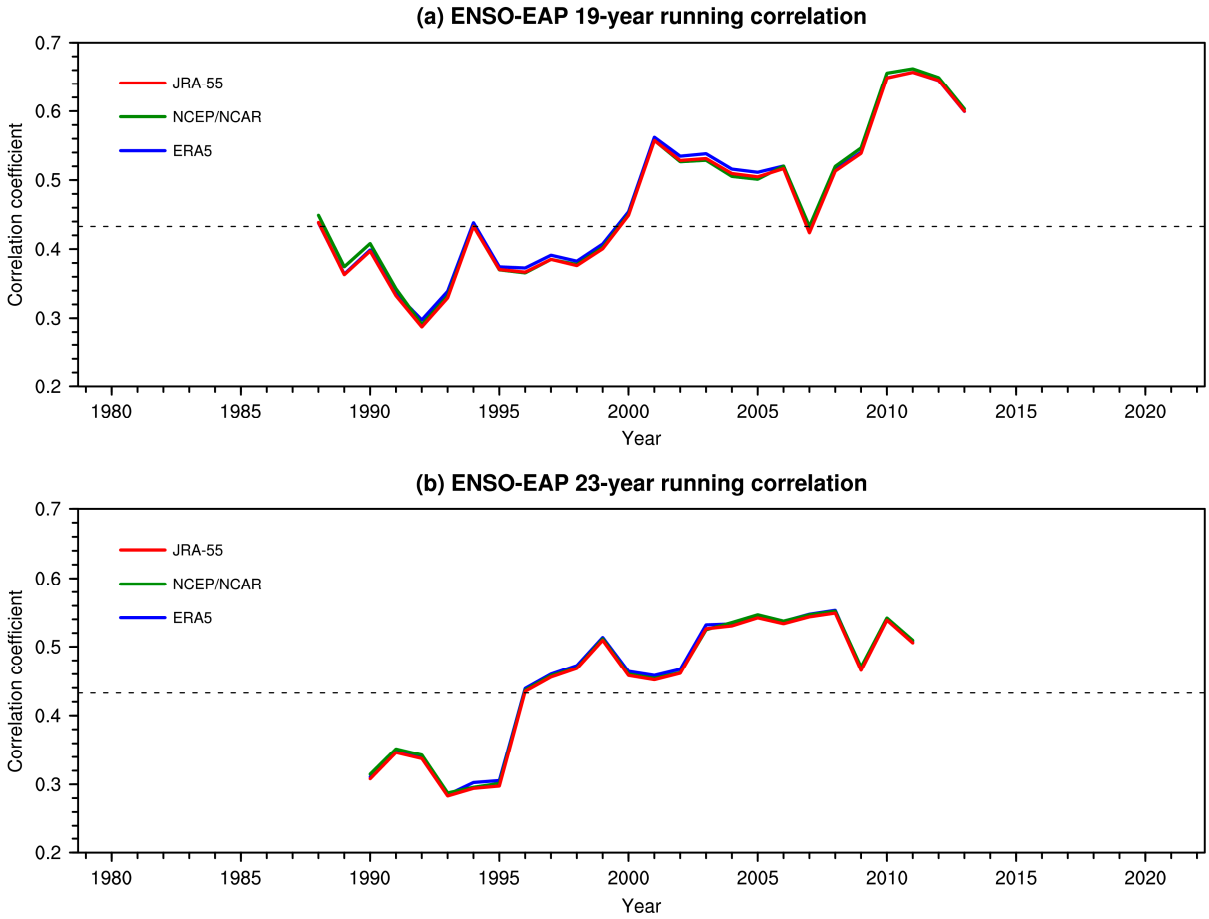

Figure S4. The (**a**) 19-year and (**b**) 23-year running correlation coefficients between the DJF Niño3.4 index and early winter EAP index during 1979–2022 based on the JRA-55 (red curve), NCEP/NCAR (green curve), and ERA5 (blue curve) reanalysis datasets. The horizontal gray dashed line indicates the 95% confidence level for the correlation.

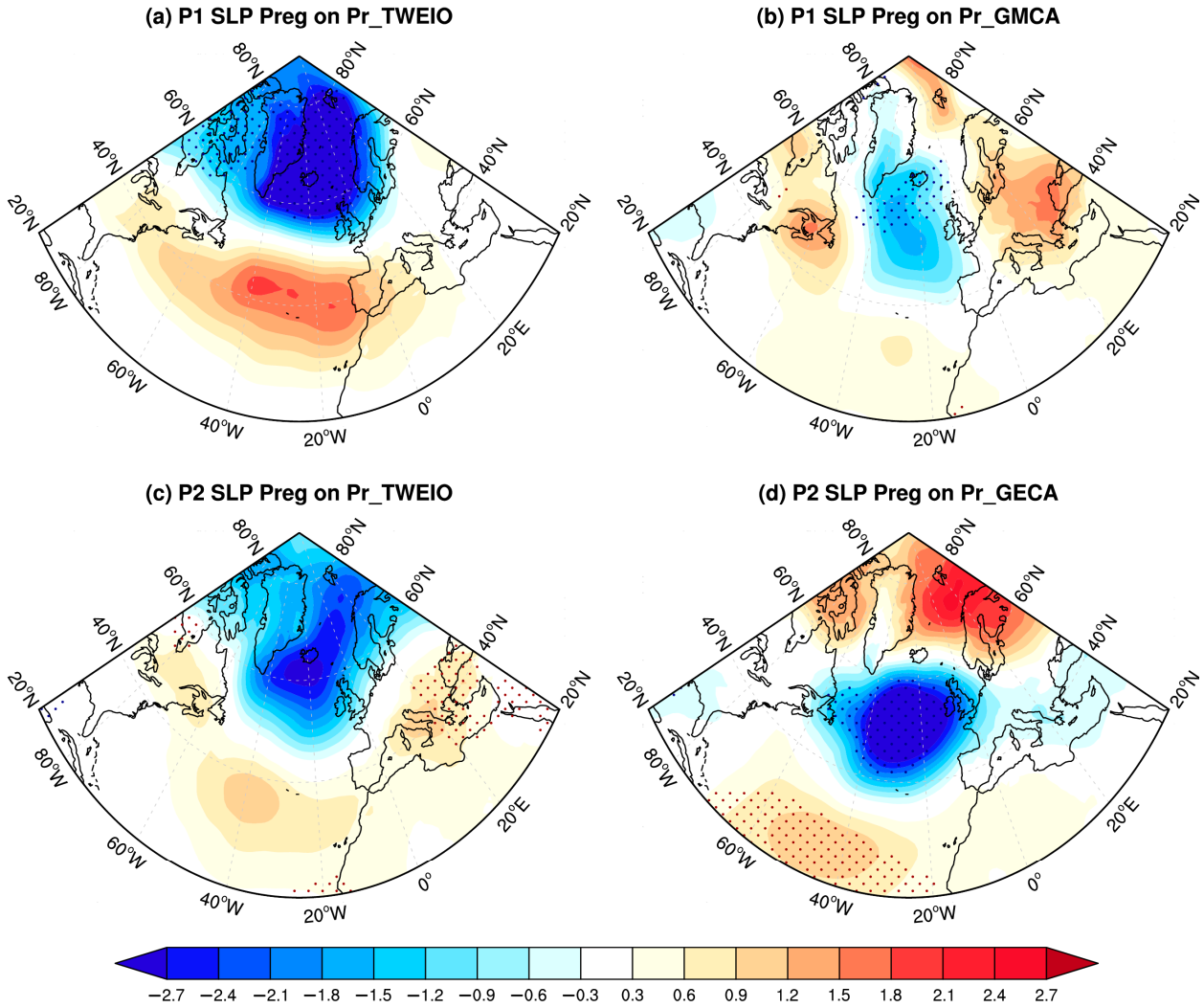

Figure S5. Partial regression coefficients of the Euro-Atlantic SLP anomalies (shading in hPa) with respect to the (**a**) Pr_TWEIO and (**b**) Pr_GMCA indices (calculated based on the CMAP precipitation dataset) during P1. (**c**)-(**d**) are the same as (**a**)-(**b**) but during P2. The dots indicate the SLP anomalies exceeding the 95% confidence level.

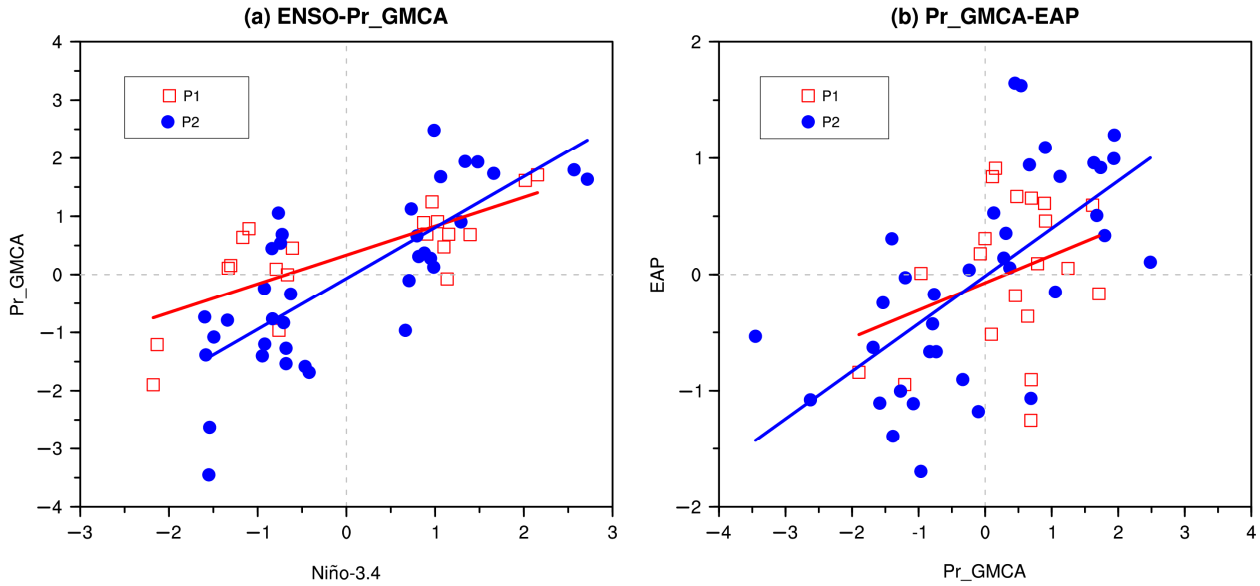

Figure S6. (**a**) Scatterplot the early winter monthly Pr_GMCA (calculated based on the CMAP precipitation dataset) and Niño-3.4 indices for the ENSO winters during P1 (red quadrate) and P2 (blue circle) with the corresponding linear regression lines. (**b**) Scatterplot the early winter monthly EAP and Pr_GMCA (calculated based on the CMAP precipitation dataset) indices for the ENSO winters during P1 (red quadrate) and P2 (blue circle). The correlation coefficients (R) are also displayed.